Materials Research. 2013; 17(2): 498-510
DOI: http://dx.doi.org/10.1590/S1516-14392014005000015
© 2014

The Columnar to Equiaxed Transition of Horizontal Unsteady-state Directionally Solidified Al–Si Alloys

***Diego B. Carvalho*[a], *Antonio L. Moreira*[a]*, *Daniel J. Moutinho*[b], *José M. Filho*[b], *Otávio L. Rocha*[b], *José E. Spinelli*[c]**

[a]*Institute of Technology, Federal University of Pará – UFPA, CEP 66075-110, Belém, PA, Brazil*
[b]*Federal Institute of Education, Science and Technology of Pará – IFPA, CEP 66093-020, Belém, PA, Brazil*
[c]*Department of Materials Engineering, Federal University of São Carlos – UFSCar, CEP 13565-905, São Carlos, SP, Brazil*

Received: July 10, 2013; Revised: December 5, 2013

Experiments were conducted to investigate the influence of thermal parameters on the columnar to equiaxed transition during the horizontal unsteady-state directional solidification of Al-Si alloys. The parameters analyzed include the heat transfer coefficients, growth rates, cooling rates, temperature gradients and composition. A combined theoretical and experimental approach is developed to determine the solidification thermal variables considered. The increasing solute content in Al-Si alloys was not found to affect significantly the experimental position of the CET which occurred for cooling rates in the range between 0.35 and 0.64 K/s for any of three alloy compositions examined. A comparative analysis between the results of this work and those from the literature proposed to analyze the CET during upward vertical solidification of Al-Si alloys is reported and the results have shown that the end of the columnar region during horizontal directional solidification is abbreviated as a result of about six times higher thermal gradient than that verified during upward unidirectional solidification of alloys investigated.

Keywords: *columnar to equiaxed transition, directional solidification, thermal parameters, unsteady-state conditions, Al-Si alloys*

1. Introduction

The origin of columnar and equiaxed grains has been the subject of numerous theoretical and experimental researches in the field of metallurgy for many years. Depending on the application, one type of grain is preferred and thus favoured, e.g. equiaxed grains in car engines and columnar grains in turbine blades as reported by Reinhart et al.[1] and McFadden et al.[2]. Equiaxed grains can nucleate and grow ahead of the columnar front causing an abrupt columnar to equiaxed transition (CET) whose prediction is of great interest for the evaluation and design of the mechanical properties of solidified products. As a consequence, it is critical for industrial applications to understand the physical mechanisms which control this transition during solidification. The CET may be sharp or gradual and it has been reported to be dependent on thermal conditions associated with the casting process, including heat transfer coefficients at the metal-mold interface (h_i), tip growth rates (V_L), thermal gradients (G_L), cooling rates (T_R), melt convection, transport of solute, alloy composition, melt superheat, mold temperature, mold design, casting size, casting geometry, and the concentration of nucleating particles, some of which vary with time and position during solidification as observed by Willers et al.[3].

The CET occurrence has been the subject of numerous studies undertaken in order to describe this phenomenon. Lack of a quantitative understanding of the relationship between casting thermal conditions and the resulting structure has limited the development of certain procedures and methods to improve the materials efficiency and performance. Although many experiments, analytical methods and numerical simulations of this process have been carried out in recent years, the mechanism of CET is still not clear. These studies highlight the importance of the relative growth of the equiaxed and columnar grains and develop expressions or numerical procedures to describe a criterion for the CET. Mahapatra and Weinberg[4], analyzing Sn-Pb alloys have observed that the position of the CET is dependent on the rate of heat extraction from the bottom of a directionally solidified ingot and independent of the melt superheat. Ziv and Weinberg[5], using an unidirectional heat transfer model, have shown that the CET occurs when G_L reaches a minimum of 0.06 °C/mm for an Al–3wt%Cu alloy, a result that confirms a gradient prediction from Hunt's solidification model[6]. Flood and Hunt[7,8] have conducted unsteady-state solidification experiments by solving a one-dimensional energy equation and tracking the position of the columnar front. The effect of alloy concentration, number

*e-mail: alsm@ufpa.br

density of equiaxed grains, h_i, and pouring temperature on the CET position were examined using the model. Wang and Beckermann[9] have developed a numerical model to calculate the CET position based on a multiphase approach, which accounts for heat and solute diffusion, as well as for grain nucleation, growth, and morphology. Ares and Schvezov[10] have performed experiments with Pb-Sn alloys directionally solidified from a chill face and observed that the CET occurs in a zone rather than in a sharp plane when G_L decreases to values ranging from –0.8 °C/cm to 1 °C/cm. Gandin[11], combining simulations furnished by a numerical model and experimental results, has proposed a CET criterion based on the position of the maximum velocity of the columnar/dendritic interface, suggesting a continuous increase in V_L up to a maximum value about two-thirds the length of the ingot, where the transition is supposed to occur. Spinelli et al.[12] have carried out experiments involving Sn–Pb alloys by changing the composition, melt superheat, and heat extraction rate at the top, promoting vertical downward directional solidification. Badillo and Beckermann[13] have developed numerical simulations of the CET in directional solidification of an Al–3wt%Cu alloy. A parametric study was performed to investigate the effects of the applied G_L and pulling speed, the seed spacing and nucleation undercooling for the equiaxed grains, and the crystalline anisotropy strength on the CET. In the study presented by Dong et al.[14], a coupled cellular automata – finite difference (CA-FD) model was applied to predict the CET in directionally solidified nickel based superalloys. The influence of G_L and V_L on CET were investigated and the results were combined on a CET map, showing that a decrease in G_L and an increase in V_L favour the CET. The experiments carried out by Nguyen-Thi et al.[15] on Al-3.5wt%Ni alloy have provided direct access to dynamical phenomena during columnar growth, and for the first time to the CET microstructure. Based on these observations, some critical parameters were measured and discussed. Banaszek et al.[16] have extended a meso-scale front-tracking model (FTM) of nonequilibrium binary alloy dendritic solidification to incorporate Kurz, Giovanola, and Trivedi (KGT) dendrite kinetics and a Scheil solidification path to predict the CET in castings in the presence of natural thermal convection. Direct simulation of equiaxed solidification has been carried out, and, when done simultaneously with columnar growth simulation, the CET was computed. Ares and Schvezov[17] have investigated experimentally the directional solidification of Al-Zn and Zn-Al alloys under different conditions of superheat and h_i. The observations indicate that the CET is the result of a competition between coarse columnar dendrites and finer equiaxed dendrites. Wu and Ludwig[18] have proposed a three-phase mixed columnar-equiaxed solidification model which considers the influence of the melt convection and grain sedimentation in the CET. Biscuola and Martorano[19] have studied the mechanical blocking of the columnar front during the CET by quantitatively, comparing the CET positions obtained with one stochastic model and two deterministic models for the unidirectional solidification of an Al-7wt%Si alloy. Silva et al.[20] have performed experiments to analyze the CET during the directional solidification of Sn–Pb alloys as a function of h_i, V_L, G_L, T_R and composition. The CET has occurred for V_L ranging from 0.08 mm/s to 0.10 mm/s and for values of G_L ranging from 0.25 K/mm to 0.90 K/mm. Noeppel et al.[21] have presented a model which is applied for simulation of the CET during solidification of Al–7wt%Si alloy under microgravity conditions. In the model, melt convection has not been taken into account and the heterogeneous nucleation of equiaxed grains was supposed to occur on nucleants characterised by a density. The objective of solidification experiments conducted by Jung et al.[22] was to understand how the formation and the evolution of the CET are influenced by the processing parameters and the natural convection in Al–3.5wt%Ni and Al–7.0wt%Si alloys. The results show that there is an oscillation of solutal concentration at the level of CET which is favoured for high T_R and low G_L. Wu et al.[23,24] have developed a model for the mixed columnar-equiaxed solidification. The main features the authors verified include nucleation of equiaxed grains ahead of the columnar tip front, CET, melt convection and sedimentation of equiaxed crystals. Ares et al.[25] have performed experiments to investigate the CET in Al-Cu alloys of different compositions which were directionally solidified. The thermal parameters studied included recalescence, G_L, V_L and T_R. The authors found that the G_L and V_L reach critical values between - 0.44 and 0.09 K/mm and between 0.67 and 2.16 mm/s, respectively, at the CET. Gueijman et al.[26] have experimentally analyzed the CET in Zn-Al and Zn-Ag alloys solidified in horizontal and vertical form, and thermal parameters such as V_L, G_L, and T_R were determined. The results showed that the CET was obtained in the vertical setup, however, it does not occur in the horizontal solidification when critical minimum gradients reach values greater than 0.1 K/mm. The model developed by Martorano et al.[27], to predict the CET during solidification of binary alloys, is based on solutal interactions between the equiaxed grains and the advancing columnar front. The model is validated by predicting the CET in unidirectional solidification involving Al-Si alloys of three different compositions. The review of CET presented by Spittle[28] considered the proposed mechanisms of equiaxed grain formation, the influence of alloy and processing conditions on the CET, criteria for the termination of columnar growth and deterministic/stochastic models for predicting the structural transition.

The effects of the direction of gravity in relation to the CET have been studied with the chill placed mainly on the bottom or top of the mold. In the case of vertical upward directional solidification the influence of the convection is minimized when solute is rejected for the interdendritic regions, providing the formation of an interdendritic liquid denser than the global volume of liquid metal. When the process is carried through vertically downward the system, it provides the melt convection which arises during the process. In the horizontal unidirectional solidification, when the chill is placed on the side of the mold, the convection in function of the composition gradients in the liquid always occurs. An interesting feature of the horizontal configuration is the gradient of solute concentration and density in vertical direction, because solute-rich liquid falls down whereas free

solvent-crystals rise due to buoyancy force. Moreover, there will also be a vertical temperature gradient in the sample as soon as the thermo-solutal convection roll emerges. In spite of these particular physical characteristics, only a few studies have reported these important effects of melt convection to the CET and rare works have been undertaken to examine experimentally the CET during the horizontal unsteady-state directional solidification of alloys.

It is well established that silicon is one of the most significant alloying elements incorporated in aluminium alloys[29,30]. Its addition is to improve castability, wear and corrosion resistance, pressure tightness, weldability, fluidity, reduce shrinkage and to render superior mechanical properties. Al-Si alloys are one of the most commonly utilized foundry alloys because they offer many advantages, therefore, they provide the most significant part of all shaped castings manufactured. If the macro and microstructures are controlled, they should have excellent mechanical properties. These alloys are generally used in engineering components that are supposed to be exposed to critical wear conditions, such as pistons, cylinder blocks and heads, water-cooled jackets, engine parts, etc. The macrostructural development of hypoeutectic Al-Si alloys has been reported in the literature, however, as reviewed, rares studies have investigated influences of thermal parameters (h_i, V_L, T_R and G_L) on CET during the horizontal unsteady-state directional solidification.

The objective of this study is to investigate the influence of thermal parameters on the CET in three hypoeutectic Al-Si alloys during the horizontal unsteady-state directional solidification in a cooled mold. A combined theoretical and experimental approach is applied to quantitatively determine the solidification thermal parameters such as h_i, V_L, T_R, and G_L which influence the structure transition. A comparative study between the results of this article and those obtained by Peres et al.[31] who studied the CET during upward vertical solidification of Al-Si hypoeutectic alloys is also presented. In this context, this study may contribute to a better understanding of the thermal characteristics and processes occurred in the Al-Si alloys during the CET. The achieved results can be used for liquid metal processing in science and industry aiming at designing of a required alloy microstructure and mechanical properties of Al-Si alloys.

2. Experimental Procedure

Experiments were carried out with Al-3wt%Si, Al-7wt%Si and Al-9wt%Si hypoeutectic alloys. The chemical compositions of metals that were used to prepare the alloys investigated are those reported in Table 1. The thermophysical properties of these alloys are summarized in Table 2. The experimental apparatus used to achieve directional solidification of Al-Si alloys, shown in Figure 1, was designed in such a way that the heat was extracted only through a water-cooled system placed in the lateral mold wall, promoting horizontal directional solidification. A stainless steel mold was used which was 110 mm long, 70 mm wide, 60 mm high and 3 mm thick. The lateral inner mold walls were covered with a layer of insulating alumina and the upper part of the mold was closed with refractory material to minimize heat losses from the mold. In order to ensure reproducibility and to favor the macrostructural transition some features of the experimental setup were standardized such as heat-extracting surface at the mold being polished, starting melt superheats in 10% above the liquidus temperature and water flow constant of 12 LPM.

The experimental procedure was as follows: the alloys were melted in situ using an electrical furnace whose heaters had their power controlled in order to permit a desired superheat to be achieved; approaching the superheat temperature, the mold was taken from the heater and set immediately on a water cooled stainless steel chill; water circulated through this cooling jacket keeping the stainless steel plate, during the solidification, at a constant

Table 1. Chemical compositions (wt pct) of metals used to prepare the Al-Si alloys.

Metal	Al	Fe	Ni	Si	P	Ca	Ti	Zn	Ga	V	Cu
Al	99.707	0.176	0.006	0.062	-	-	0.009	0.007	0.012	0.011	0.005
Si	0.109	0.316	0.010	99.596	0.010	0.021	0.046	-	-	-	-

Table 2. Casting material used for experimentation and the corresponding thermophysical properties[31].

Properties	Thermal conductivity	Specific heat	Density	Latent heat of fusion	Solute diffusivity	Solidus temperature	Liquidus temperature	Partition coefficient	Liquidus slope
Symbol/ units	K_S [W/m.K] (solid) K_L [W/m.K] (liquid)	c_S [J/kg.K] (solid) c_L [J/kg.K] (liquid)	ρ_S [kg/m^3] (solid) ρ_L [kg/m^3] (liquid)	L [J/kg]	D [m^2/s]	T_S [°C]	T_L [°C]	k_O	m_L (K/wt pct)
Al-3wt.%Si	121 91	963 1084	2695 2385	389187	3×10^{-9}	577	644	0.13	6
Al-7wt.%Si	90 90	963 1080	2680 2394	397440	3×10^{-9}	577	610	0.13	6
Al-9wt.%Si	81 89	963 1078	2670 2399	405548	3×10^{-9}	577	604	0.13	6

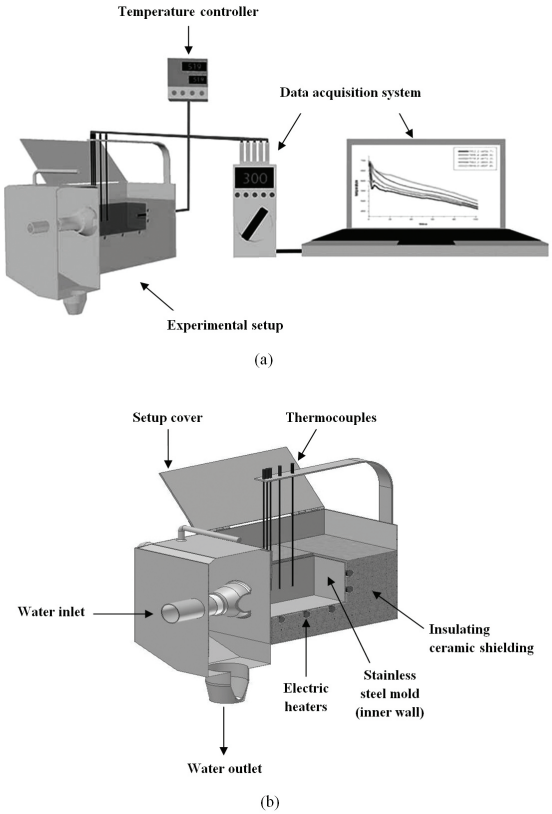

Figure 1. (a) Schematic representation of the experimental apparatus for directional solidification; (b) Furnace schematic showing thermocouples located at different positions from the metal-cooling chamber interface.

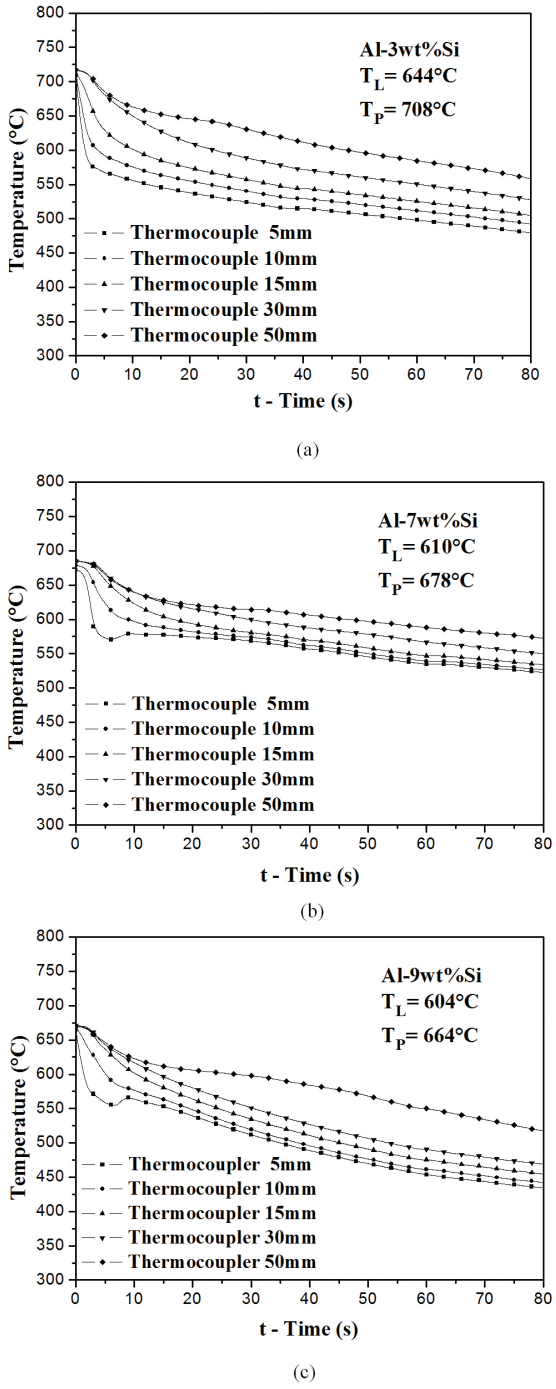

Figure 2. Experimental thermal responses of temperature vs. time for five thermocouples located at different positions from the metal-cooling chamber interface. T_p is the initial melt temperature.

temperature of about 25 °C, thus inducing a longitudinal heat transfer from the mold. The thermal contact condition at the metal/mold interface was also standardized with the heat-extracting surface being polished. Solidification occurred dendritically from the lateral chill surface, forming a columnar structure.

Continuous temperature measurements were made during solidification at different positions in the casting and the data were acquired automatically. For the measurements, a set of five fine type K thermocouples accurately located with respect to the metal/mold interface was used, as shown by the schematic representation presented in Figure 1b. The thermocouples were sheathed in 1.6 mm diameter steel tubes, and positioned at 5, 10, 15, 30 and 50 mm from the heat-extracting surface. The thermocouples were calibrated at the melting point of aluminum, exhibiting fluctuations of about 1.0 °C, and connected by a data acquisition system and stored on a computer. Previous measurements of the temperature field were carried out confirming that the described experimental setup fulfills the requirement of a unidirectional heat flow in horizontal direction.

Each ingot was sectioned along its longitudinal direction, which is parallel to both the sample axis and the direction of solidification. After this, the metallographic specimens were mechanically polished with abrasive papers and subsequently etched with an acid solution composed of 5 ml H_2O, 60 ml HCl, 30 ml HNO_3 and 5 ml HF to reveal the macrostructures. Etching was performed at a temperature between 30 °C and 35 °C during approximately 10 minutes. The position of the CET was clearly delineated by visual

observation and optical microscopy on the etched surface, and the distance from the side of the sample was measured.

Special care was taken to achieve well-defined h_i values. Therefore, in this paper, the results of experimental thermal analysis in alloys investigated were compared with theoretical values given by a finite difference heat flow model developed by Santos et al.[32-34] to determine h_i. This method makes a complete mathematical description of the physics of the process and is supported by temperature measurements at known locations inside the heat conducting body. The process at each time step included the following: a suitable initial value of h_i is assumed and with this value, the temperature of each reference location in casting at the end of each time interval Δt is simulated by the numerical model. The correction in h_i at each interaction step is made by a value Δh_i and new temperatures are estimated $[T_{est}(h_i + \Delta h_i)]$ or $[T_{est}(h_i - \Delta h_i)]$. With these values, sensitivity coefficients ($\emptyset$) are calculated for each interaction, given by:

$$\phi = \frac{T_{est}(h_i + \Delta h_i) - T_{est}(h_i)}{\Delta h_i} \quad (1)$$

The procedure determines the value of h_i, which minimizes an objective function defined by:

$$F(h_i) = \sum_{i=1}^{n} \left(T_{est} - T_{\exp}\right)^2 \quad (2)$$

where T_{est} and T_{exp} are the estimated and the experimentally measured temperatures at various thermocouples locations and times, and n is the iteration stage. An automatic search has selected the best theoretical-experimental fit from a range of transient heat transfer coefficients profiles. In the heat transfer model it is assumed that heat flow is linear parallel to the ingot axis. The interfacial heat transfer coefficients have been expressed as a power function of time, given by the general form $h_i = C\,(t)^{-n}$ where h_i (W/mK), t (s) and C and n are constants which depend on mold material, superheat and alloy composition.

The numerical model employed for h_i theoretical estimation was selected from the literature as the most appropriate model for representing the solidification conditions considered in this study. Moreover, it has been frequently used by other authors in researching unidirectional solidification in downward vertical[12,33-35], horizontal[32-34,36] and rotary systems[37], which produce melt convection effects.

Simulated h_i curves were used in another numerical solidification model[12] in order to calculate theoretical values of V_L, T_R, and G_L which are usually associated with CET. In the numerical model, the values of thermal parameters V_L, T_R, and G_L are explicitly calculated at each time increment (0.001 s) of the simulation.

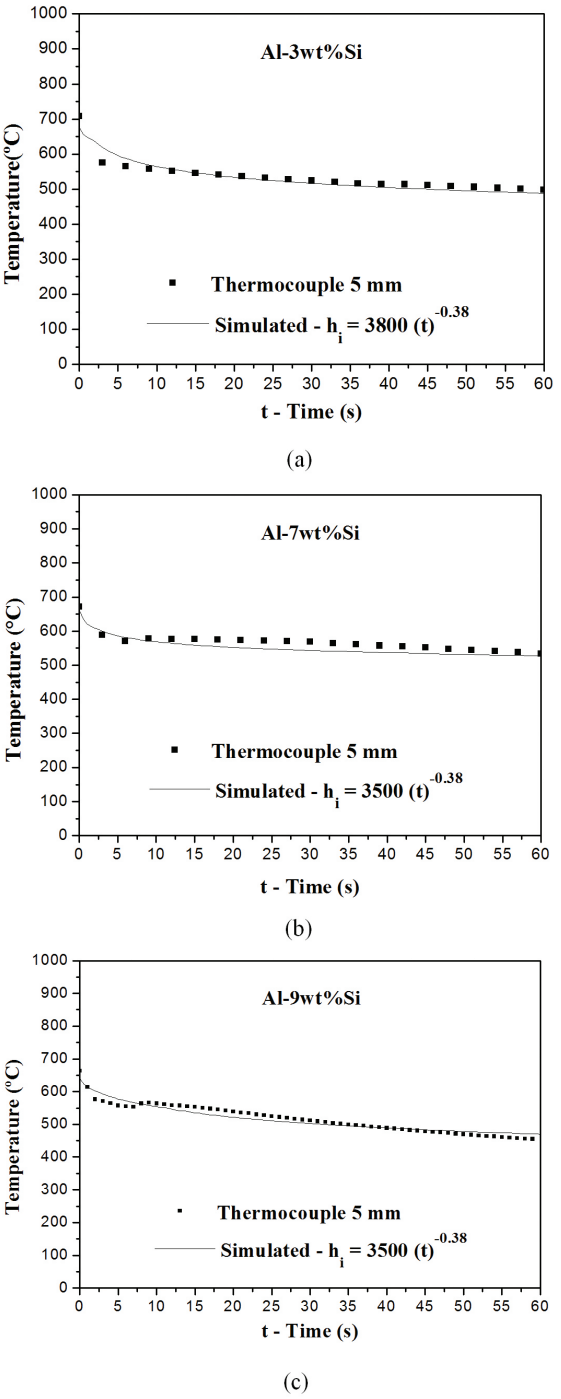

Figure 3. Simulated and measured temperature responses of thermocouple at position 5 mm from the heat-extracting surface of Al-Si alloys investigated.

3. Results and Discussion

3.1. *Interfacial heat transfer coefficient (h_i)*

Typical examples of experimental cooling curves for the five thermocouples inserted into the casting, during solidification of the three alloys examined in the present study are shown in Figure 2. For determination of the values of h_i, it was used the referring thermal profile to the thermocouple next to the cooled base (5 mm), position for which eventual heat losses by lateral walls of the mold is more improbable. Experimental thermal responses were compared to those simulated numerically by using transient

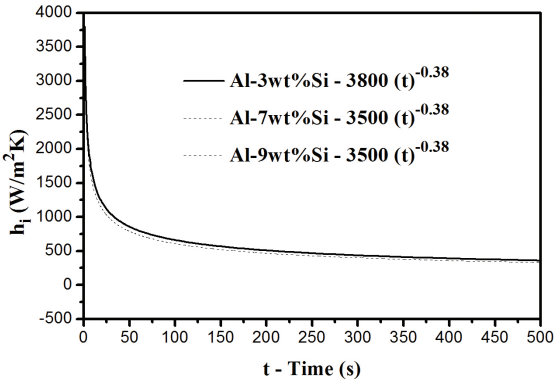

Figure 4. Evolution of the metal-mold interfacial heat transfer coefficients as a function of time.

h_i profiles which provide best curve fitting, as shown in Figure 3. The time dependence of overall h_i during the course of different experiments of horizontal directional solidification of hypoeutectic Al-Si alloys in polished cooled molds are shown in Figure 4. It can be seen that the h_i profile is essentially the same for any Al-Si alloy examined. Solidification contraction associated with increasing solute concentration in conditions of horizontal growth were not found to contribute to the detachment of ingot surface from the cooled mold in the early beginning of solidification not producing, therefore, a greater thermal resistance. It is noticed, still, for all the compositions, a significant reduction of h_i values in the initial instants of the process, mainly in the first 25 seconds of the total time of solidification. From this time until the 100 seconds, a gradual reduction of h_i values occurs. After this time, it remains practically constant until the end of the solidification.

3.2. *Columnar to Equiaxed Transition (CET)*

It is well established that the macrostructure of cast ingots generally consists of four distinct zones. These are the chill zone (observed in the vicinity of the mould walls), the columnar zone (composed of elongated grains whose growth is preferentially oriented in a direction close to the heat flux), the equiaxed zone (located in the central part of the casting in which the grains grow in all space directions) and the surface dendrite layer formed on a metal-air interface, respectively. All four zones may or may not be present in a particular case. When a casting contains columnar and equiaxed grains, the columnar-to-equiaxed transition (CET) is usually narrow.

The directionally solidified structures of Al-Si alloys are shown in Figure 5. The macrostructures consisted of elongated columnar grains, aligned approximately parallel to the direction of the heat flow, as well as of equiaxed grains of varying extent and random orientations. It can be noticed that approximately sixty percent of the Al-Si ingots are composed of a columnar dendritic grain structure, after which it is observed a region of equiaxed dendritic grains. No chill region is found in the solidified structures. If a surface dendrite layer is formed at the upper part of the Al-Si ingots, it is not clearly evident in the macrostructures. A CET is observed at the shared boundaries in which the two zones meet. The basic feature of the transition shown by these macrostructures is that the CET is sharp, i.e., there is clear evidence that the structural transformation occurred along a plane parallel to the chill wall because of the high density of rapidly growing equiaxed grains. The sharpness of the CET is observed not to vary in the Al-Si ingots as a function of the composition. A particular interesting behavior concerning progress of solidification has been observed for the Al-Si alloys experimentally examined in this study. In the experiments, varying alloy composition was expected to influence the extent of the equiaxed zone in a systematic way; however, the solute content was not found to affect significantly the experimental position of the structure transition, which occurred essentially at the same position for the experiments carried out in this study. The CET occurred at 68, 65 and 65 mm, measured from the metal/cooling chamber interface, respectively, for Al-3wt%Si, Al-7wt%Si and Al-9wt%Si alloys. A tolerance of ±1 mm was quoted with each CET position. These results are in agreement with observations reported by Peres et al.[31] and Gandin[38] experiments with Al-Si alloys directionally solidified. Peres et al.[31] have conducted experiments to analyze the upward unsteady-state directional solidification of Al–Si alloys (3, 5, 7 and 9 wt% Si) in a water cooled stainless steel mold. A combined theoretical and experimental approach was developed to quantitatively determine solidification thermal variables such as transient metal/mold heat transfer coefficients, tip growth rates, thermal gradients, tip cooling rates and local solidification time. The observation of the macrostructures has shown that the CET occurred essentially at the same position from the casting surface for any alloy experimentally examined. Gandin[38] has performed upward unsteady-state directional solidification experiments on Al-3wt%Si, Al-7wt%Si and Al-11wt%Si alloys in a water cooled copper chill. After comparing CET positions the author observed that the columnar length was found to increase slightly with decreasing the solute content.

3.3. *Solidification thermal parameters (V_L, T_R, and G_L)*

The CET is dependent on solidification thermal parameters such as V_L, T_R, and G_L all of which vary with time and position during solidification. It is well known that it is very difficult to measure these parameters at the CET accurately, using thermocouples, since the position of the transition is not known before each experimental test. In order to determine more accurate values of these parameters the results of experimental thermal analysis have been used to determine the displacement of the liquidus isotherm, i.e., the thermocouples readings have also been used to generate a plot of position from the metal/mold interface as a function of time corresponding to the liquidus front passing by each thermocouple. A curve fitting technique on such experimental points has generated power functions of position as a function of time. Experimental positions of liquidus isotherms as a function of time are shown in Figure 6 compared with the theoretical results furnished by the numerical solidification model, which

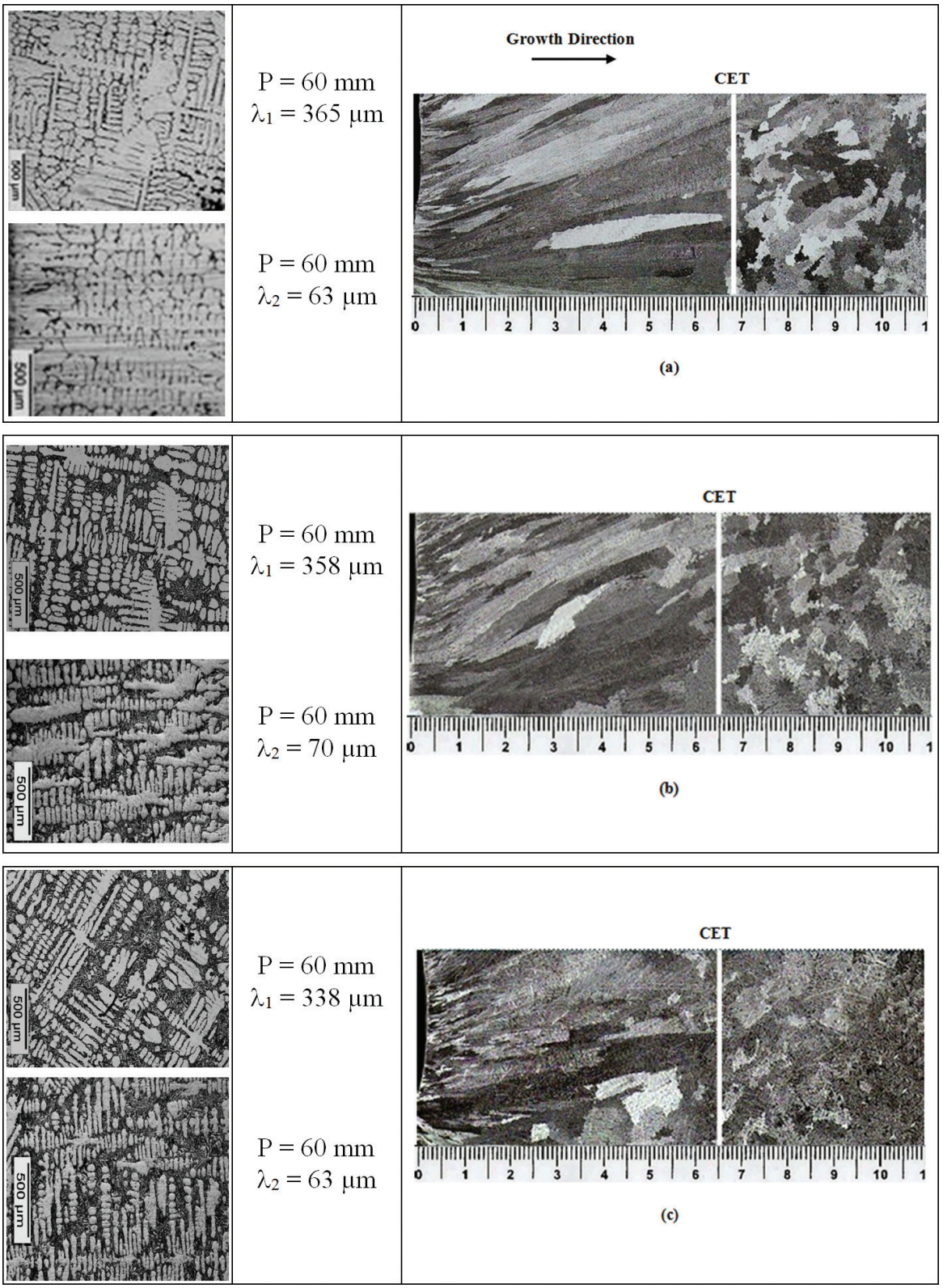

Figure 5. Solidification macrostructures, CET positions (cm), and corresponding primary and secondary spacings: (a) Al–3wt%Si; (b) Al–7wt%Si; (c) Al–9wt%Si.

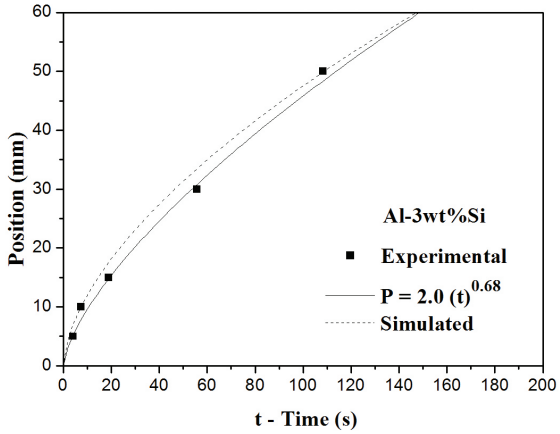

(a)

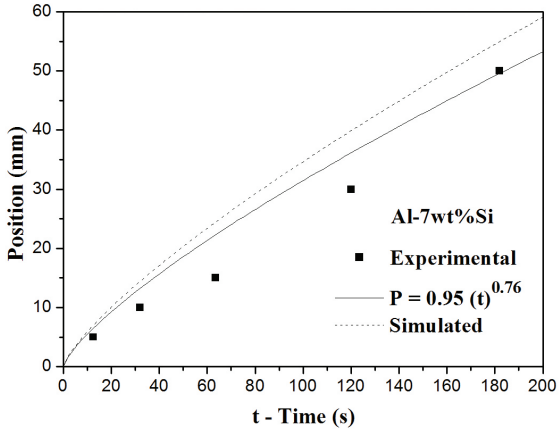

(b)

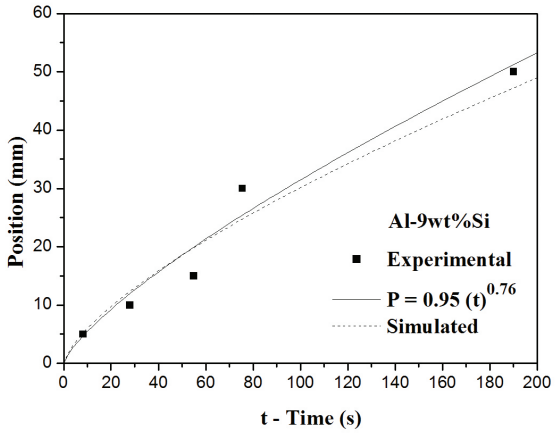

(c)

Figure 6. Experimental position of liquidus isotherm from the metal/mold interface as function of time.

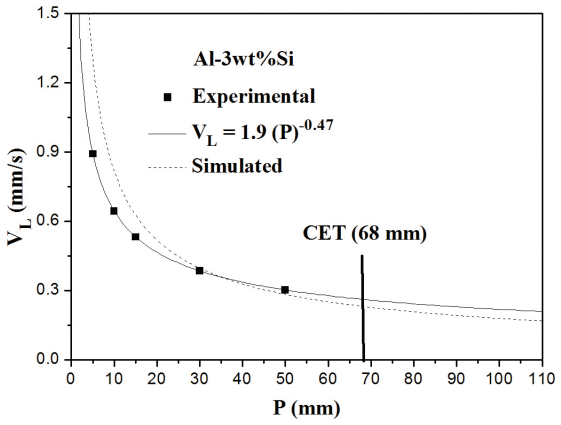

(a)

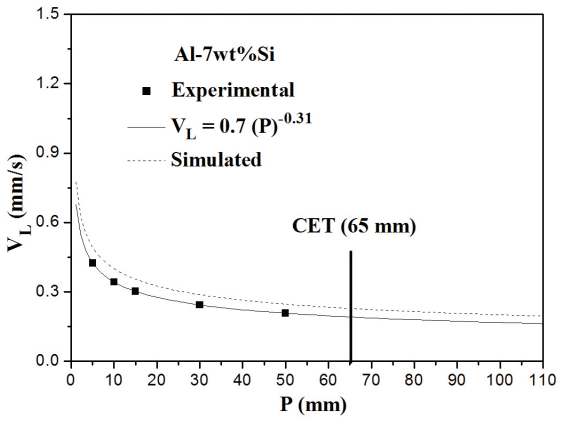

(b)

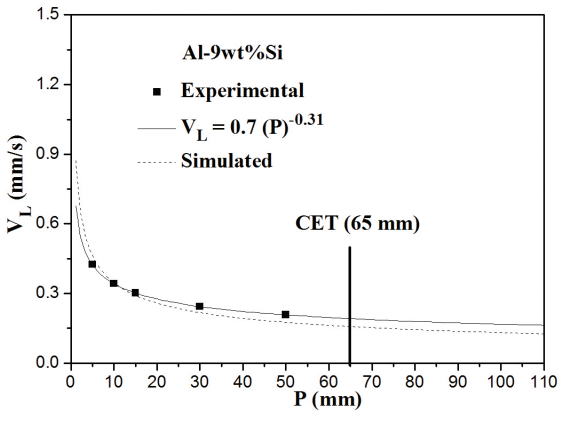

(c)

Figure 7. Tip growth rate as a function of position from the metal/mold interface for Al-Si alloys during horizontal solidification.

used the corresponding values of the transient heat-transfer coefficient presented in Figure 4. A good agreement has been observed between the experimental results and numerical values for any alloy Al-Si investigated.

The derivative of this function with respect to time has yielded values for V_L. Figure 7 shows typical comparisons between experimental and numerical predictions[12] of V_L. The data acquisition system, in which temperature readings are collected at a frequency of 0.5 s, permits accurate determination of the slope of the experimental cooling curves. The T_R values were calculated by considering the thermal data recorded immediately after the passing of

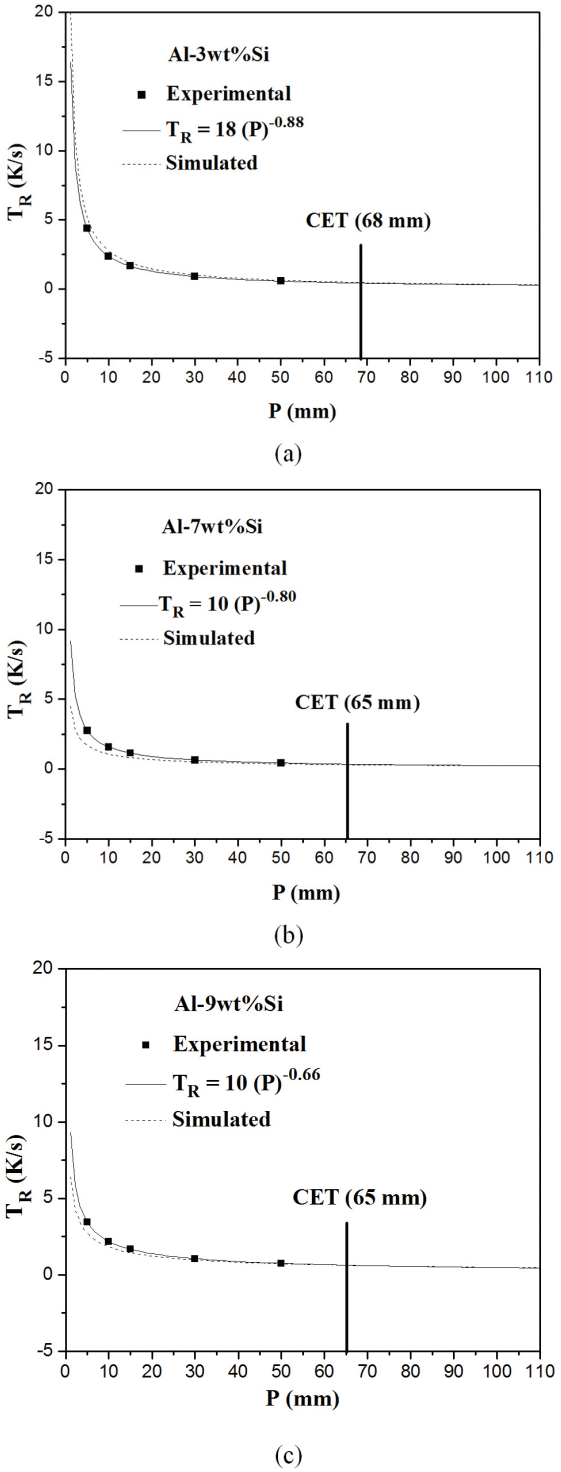

Figure 8. Tip cooling rate as a function of position from the metal/mold interface for Al-Si alloys during horizontal solidification.

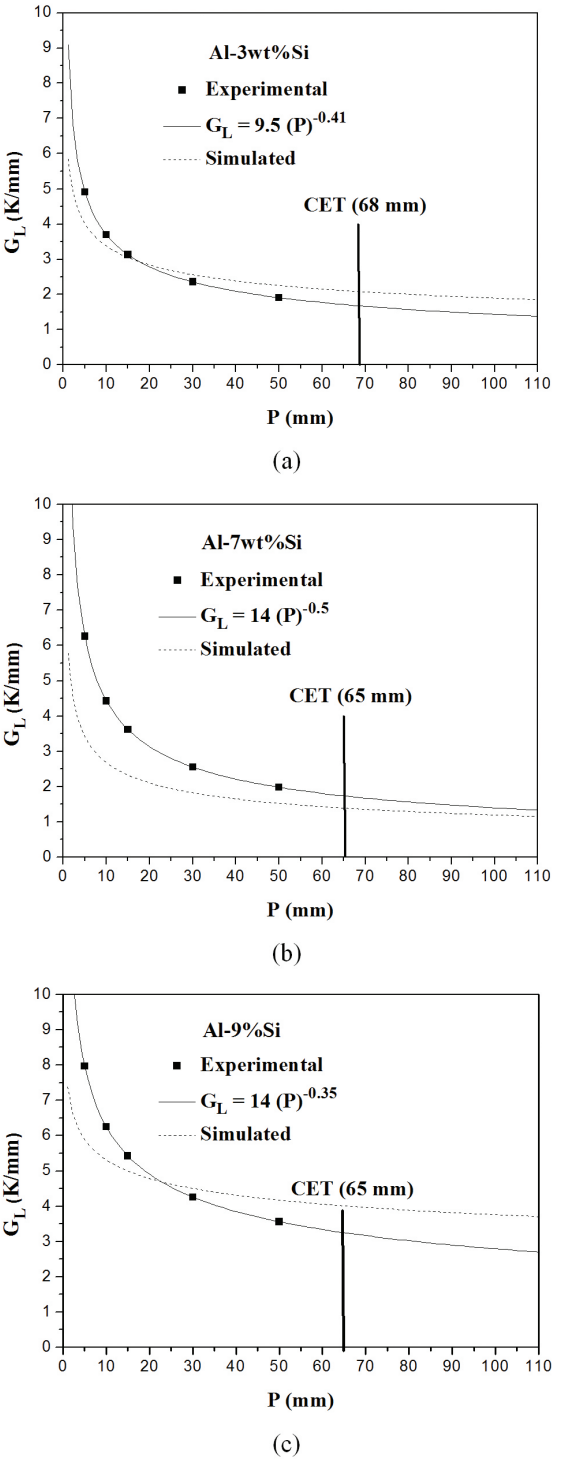

Figure 9. Temperature gradient as a function of position from the metal/mold interface for Al-Si alloys during horizontal solidification.

the liquidus front by each thermocouple whose values are compared with theoretical predictions furnished by the numerical model[12] in Figure 8. A good agreement can be observed between the experimental values of V_L and T_R and those numerically simulated for all the alloys examined.

Finally, theoretical results of G_L as a function of position from the chill provided by the numerical model[12] are shown in Figure 9 in which it can be seen that G_L decreases with distance from the metal/mold interface, as expected. Generally speaking, a good agreement has been observed

between the experimental values found for these thermal parameters and those numerically simulated for all the experiments. The experimental and corresponding numerical power laws determined in this work are presented in Table 3.

3.4. *CET position*

Experimental and numerical results of V_L, T_R and G_L at each CET position are listed in Table 4. The obtained results in the present work do not give support to a CET criteria based individually on a particular variable. A number of CET criteria[5,10,11,25,26] found in the literature neglect in their analysis the existence of melt convection ahead solidification front and its effects on the blockage of the columnar front. In these cases, a single solidification thermal variable may be established as the critical one for the macrostructural transition to happen. This is absolutely not the case of the present investigation. In our present study, vigorous natural convection is due to thermal and solutal gradients within the molten alloy on both transverse and longitudinal directions in relation to the solidification progress. Such complex configuration is responsible, for instance, by some tilting upwards on the columnar growth as solidification progresses as can be clearly seen in Figure 5a and 5b. Table 4 depicts that CET is not controlled by a critical value of a single thermal variable (V_L, T_R and G_L) for any of the three alloy compositions.

The maximum velocity criterion proposed by Gandin[11,38] concerning the directional solidification of Al-Si alloys seems to be in contradiction with the present results due to the fact that the obtained growth rates during horizontal solidification of the Al-Si alloys are proved to decrease up to a minimum value as the distance from water-cooled mold surface is increased (see Figure 7).

The structural transition has occurred, for Al-Si alloys examined, for tip growth rates ranging from 0.19 to 0.26 mm/s making it clear that a CET criterion based only on tip growth rate is not consistent with the experimental values. It is noticed, still, that the experimental position of the CET occurred for cooling rates and temperature gradients in the melt ahead of the liquidus isotherm in the range between 0.35 to 0.64 K/s and 1.68 to 3.25 K/mm, respectively, for any of three alloy compositions examined. Comparison with other experimental results from the literature also do not give support to a CET criterion based only on coolig rate or thermal gradient.

The results of the present experimental investigation and those obtained by Peres et al.[31] concerning values of V_L, T_R, and G_L at the CET position during solidification of Al-Si alloys in systems with different configurations are summarized in Table 5. It can be observed that the average values of these parameters show that the macrostructure transition obtained by Peres has been undertaken under conditions of higher values of V_L and lower values of T_R and G_L in the melt at the liquidus temperature when compared with those reported in the present study. In both cases, the alloy solute content was not found to affect significantly the experimental position of the structure transition, which occurred essentially at the same position in each set of experiments. It is very important to observe that the length of the columnar region during horizontal unidirectional solidification is abbreviated in one third. A six times higher G_L average value for CET (2.22 K/mm) was derived concerning horizontal solidification than that verified during upward unidirectional solidification (0.39 K/mm) of Al-Si alloys which has been performed under thermally and solutally stable conditions, i.e., cooling from the bottom of the casting ensures that the liquid is stable with regard to thermally derived density gradients in the liquid. It is usually assumed that the effect of the natural convection in the liquid can be neglected in this case[31,39].

According to Bogno et al.[40], however, even thermal and solutal stabilising configurations can experience strong convection flow in the melt due to transverse gradients. This kind of effect is quite expected for horizontal solidification setup. Lower V_L values may become such effect even more noticeable. The mean value found for V_L corresponding to horizontal solidification (0.21 mm/s) is about two times lower than average V_L found for vertically upward CET (0.45mm/s). This is probably due to accumulation of solute in the bottom part of the casting during horizontal growth. As a consequence, the concentration gradient in the liquid phase ahead of the solid-liquid interface is gradually reduced, decreasing not only growth rate but also mushy zone length[40]. On the other hand, according to Hellawell and

Table 3. Experimental and numerical power laws obtained in the present study.

Alloys	Experimental power laws				Numerical power laws			
Al-3wt%Si	$P = 2(t)^{0.68}$	$V_L = 1.9(P)^{-0.47}$	$T_R = 18(P)^{-0.88}$	$G_L = 9.5(P)^{-0.41}$	$P = 3(t)^{0.60}$	$V_L = 3.74(P)^{-0.66}$	$T_R = 22.4(P)^{-0.91}$	$G_L = 6(P)^{-0.25}$
Al-7wt%Si	$P = 0.95(t)^{0.76}$	$V_L = 0.7(P)^{-0.31}$	$T_R = 10(P)^{-0.80}$	$G_L = 14(P)^{-0.50}$	$P = 1(t)^{0.77}$	$V_L = 0.80(P)^{-0.30}$	$T_R = 4.8(P)^{-0.65}$	$G_L = 6(P)^{-0.35}$
Al-9wt%Si	$P = 0.95(t)^{0.76}$	$V_L = 0.7(P)^{-0.31}$	$T_R = 10(P)^{-0.66}$	$G_L = 14(P)^{-0.35}$	$P = 1.2(t)^{0.70}$	$V_L = 0.91(P)^{-0.42}$	$T_R = 6.8(P)^{-0.57}$	$G_L = 7.5(P)^{-0.15}$

Table 4. Experimental and numerical results for the solidification thermal parameters associated to the CET position.

Alloys	CET position (mm)	Thermal parameters					
		V_L (mm/s)		T_R (K/s)		G_L(K/mm)	
		Experimental	Numerical	Experimental	Numerical	Experimental	Numerical
Al-3wt%Si	68	0.26	0.23	0.44	0.48	1.68	2.09
Al-7wt%Si	65	0.19	0.23	0.35	0.32	1.74	1.39
Al-9wt%Si	65	0.19	0.16	0.64	0.63	3.25	4.01
Average	66	0.21	0.21	0.48	0.48	2.22	2.50

Table 5. Solidification thermal parameters associated to the CET position for the present experiments and those conducted by Peres et al.[31] for Al-Si alloys.

Author	System	Heat flow conditions	Heat extracting surface	Melt convection	Alloys	Superheat (K)	h_i (W/m^2K)	V_L (mm/s)	T_R (K/s)	G_L (K/mm)	CET position (mm)
Peres et al.	upward vertical	unsteady state	water cooled stainless steel	No	Al-3wt%Si	2	$4800(t)^{-0.09}$	0.50	0.16	0.32	94
					Al-7wt%Si	2	$3900(t)^{-0.09}$	0.45	0.15	0.33	95
					Al-9wt%Si	2	$3300(t)^{-0.09}$	0.39	0.20	0.52	97
					Average			0.45	0.17	0.39	95
This work	horizontal	unsteady state	water cooled stainless steel	Yes	Al-3wt%Si	64	$3800(t)^{-0.38}$	0.26	0.44	1.68	68
					Al-7wt%Si	61	$3500(t)^{-0.38}$	0.19	0.35	1.74	65
					Al-9wt%Si	60	$3500(t)^{-0.38}$	0.19	0.64	3.25	65
					Average			0.21	0.48	2.22	66

collaborators[41] the initial dendritic mushy region is assumed to be the most potent source of solid fragments. Transport and survival of such fragments seem to be favored by higher fluid flow rates as those experienced during horizontal growth, even though smaller undercooled zone in front of dendrite tips is available as a function of higher G_L values. This may inhibit the subsequent growth of fragments. In the mushy region there are millions of potential side-arm fragments, and only a fraction of these need to escape to be effective in the ahead open liquid regions. Narrow mushy zone lenght seems to assist transportation of fragments toward the open melt by natural convection. In the case of horizontally solidified Al-Si alloy castings, the resulting melt convection improves chance of fragments survival than it would in a motionless liquid, as stressed by Hellawell et al.[41]. The blockage of columnar grains is shortened in the case of horizontal growth with the hypoeutectic Al-Si alloys, suddenly happening for an average T_R three times higher (0.48 K/s) than that corresponding to the CET occurred on upward vertical growth (0.17 K/s). Approaches based on the adoption of critical thermal solidification parameters corresponding to CET are not adequate for hypoeutectic Al-Si alloys considering not only the conditions performed by Peres et al.[31] using a stable configuration regarding to thermal and solutal natural flow but also the solidification conditions observed in the present study.

4. Conclusions

Experiments were conducted in order to study the CET occurrence during the horizontal unsteady-state directional solidification in a cooled mold of three hypoeutectic Al-Si alloys. The following main conclusions are derived from the present investigation:

a) The basic feature of the CET shown by the macrostructures is that the transition is sharp, i.e., the columnar-to-equiaxed transformation occurs rapidly along a plane parallel to the chill wall;
b) There is no relationship observed between the extent of the equiaxed region in the ingots and alloy composition, i.e., the increasing solute content in Al-Si alloys was not found to affect significantly the experimental position of the CET;
c) The structure transition occurred at 68, 65 and 65 mm measured from the metal/cooling chamber interface, respectively, for Al-3wt%Si, Al-7wt%Si and Al-9wt%Si alloys;
d) The h_i profile is essentially the same for any alloy examined, i.e., solidification contraction associated with increasing solute concentration in conditions of horizontal growth were not found to contribute to the detachment of ingot surface from the cooled mold in the early beginning of solidification not producing, therefore, a greater thermal resistance;
e) Generally speaking, a good agreement has been observed between the experimental values of V_L, T_R and G_L and those numerically simulated for all the experiments;
f) The structural transition has occurred for tip growth rates ranging from 0.19 to 0.26 mm/s. The experimental position of the CET has occurred for cooling rates and temperature gradients in the range between 0.35 to 0.64 K/s and 1.68 to 3.25 K/mm, respectively, for any of three alloy compositions examined;
g) The observed results do not give support to a CET criteria based individually on a particular variable;
h) The resulting melt convection seems to favor the end of the columnar region during horizontal unidirectional solidification which is abbreviated as a result of a six times higher G_L than that verified during upward unidirectional solidification of alloys examined in this work.

Acknowledgements

The authors acknowledge the financial support provided by IFPA (Federal Institute of Education, Science and Technology of Pará) and UFPA (Federal University of Pará), Brazil. C.M. Macedo de Macedo, from the Federal University of Pará, Brazil, is also acknowledged for his careful reading of the manuscript.

References

1. Reinhart G, Mangelinck-Noël N, Nguyen-Thi H, Schenk T, Gastaldi J, Billia B et al. Investigation of columnar-equiaxed transition and equiaxed growth of aluminium based alloys by x-ray radiography. *Materials Science and Engineering A*. 2005; 413-414:384-388. http://dx.doi.org/10.1016/j.msea.2005.08.197
2. McFadden S, Browne DJ and Gandin CA. A comparison of columnar-to-equiaxed transition prediction methods using simulation of the growing columnar front. *Metallurgical and Materials Transactions A*. 2009; 40A:662-672.
3. Willers B, Eckert S, Michel U, Haase I and Zouhar G. The columnar-to-equiaxed transition in Pb-Sn alloys affected by electromagnetically driven convection. *Materials Science and Engineering A*. 2005; 402:55-65. http://dx.doi.org/10.1016/j.msea.2005.03.108
4. Mahapatra RB and Weinberg F. The columnar to equiaxed transition in tin-lead alloys. *Metallurgical Transactions*. 1987; 18B:425-432. http://dx.doi.org/10.1007/BF02656163
5. Ziv I and Weinberg F. The columnar-to-equiaxed transition in AI 3pct Cu. *Metallurgical Transactions B*. 1989; 20B:731-734.
6. Hunt JD. Steady state columnar and equiaxed growth of dendrites and eutetic. *Materials Science and Engineering*. 1984; 65:75-83. http://dx.doi.org/10.1016/0025-5416(84)90201-5
7. Flood SC and Hunt JD. Columnar and equiaxed growth i. a model of a columnar front with a temperature dependent velocity. *Journal of Crystal Growth*. 1987; 82:543-551. http://dx.doi.org/10.1016/0022-0248(87)90346-0
8. Flood SC and Hunt JD. Columnar and equiaxed growth ii. equiaxed growth ahead of a columnar front. *Journal of Crystal Growth*. 1987; 82:552-560. http://dx.doi.org/10.1016/0022-0248(87)90347-2
9. Wang CY and Beckermann C. Prediction of columnar to equiaxed transition during diffusion-controlled dendritic alloy solidification. *Metallurgical and Materials Transactions A*. 1994; 25A:1081-1093.
10. Ares AE and Schvezov CE. Solidification parameters during the columnar-to-equiaxed transition in lead-tin alloys. *Metallurgical and Materials Transactions*. 2000; 31A:1611-1625. http://dx.doi.org/10.1007/s11661-000-0171-6
11. Gandin CA. From constrained to unconstrained growth during directional solidification. *Acta Materialia*. 2000; 48:2483-2501. http://dx.doi.org/10.1016/S1359-6454(00)00070-7
12. Spinelli JE, Ferreira IL and Garcia A. Influence of melt convection on the columnar to equiaxed transition and microstructure of downward unsteady-state directionally solidified Sn-Pb alloys. *Journal of Alloys and Compounds*. 2004; 384:217-226. http://dx.doi.org/10.1016/j.jallcom.2004.04.098
13. Badillo A, Beckermann C. Phase-field simulation of the columnar-to-equiaxed transition in alloy solidification. *Acta Materialia*. 2006; 54:2015-2026. http://dx.doi.org/10.1016/j.actamat.2005.12.025
14. Dong HB, Yang XL, Lee PD and Wang W. Simulation of equiaxed growth ahead of an advancing columnar front in directionally solidified Ni-based superalloys. *Journal of Materials Science*. 2004; 39:7207-7212. http://dx.doi.org/10.1023/B:JMSC.0000048733.96958.c3
15. Nguyen-Thi H, Reinhart G, Mangelinck-Noël N, Jung H, Billia B, Schenk T et al. In-situ and real-time investigation of columnar-to-equiaxed transition in metallic alloy. *Metallurgical and Materials Transactions A*. 2007; 38A:1458-1464.
16. Banaszek J, McFadden S, Browne DJ, Sturz L and Zimmermann G. Natural convection and columnar-to-equiaxed transition prediction in a front-tracking model of alloy solidification. *Metallurgical and Materials Transactions A*. 2007; 38A:1476-1484.
17. Ares AE and Schvezov CE. Influence of solidification thermal parameters on the columnar-to-equiaxed transition of aluminum-zinc and zinc-aluminum alloys. *Metallurgical and Materials Transactions A*. 2007; 38A:1485-1499.
18. Wu M and Ludwig A. Using a three-phase deterministic model for the columnar-to-equiaxed transition. *Metallurgical and Materials Transactions A*. 2007; 38A:1465-1475.
19. Biscuola VB and Martorano MA. Mechanical blocking mechanism for the columnar to equiaxed transition. *Metallurgical and Materials Transactions A*. 2008; 39A:2885-2895.
20. Silva JN, Moutinho DJ, Moreira AL, Ferreira IL and Rocha OL. The columnar to equiaxed transition during the horizontal directional solidification of Sn-Pb alloys. *Journal of Alloys and Compounds*. 2009; 478:358-366. http://dx.doi.org/10.1016/j.jallcom.2008.11.026
21. Noeppel A, Budenkova O, Zimmermann G, Sturz L, Mangelinck-Noël N, Jung H et al. Numerical modelling of columnar to equiaxed transition-application to microgravity experiments. *International Journal of Cast Metals Research*. 2009; 22:34-38. http://dx.doi.org/10.1179/136404609X367272
22. Jung H, Mangelinck-Noël N, Nguyen-Thi H and Billia B. Columnar to equiaxed transition during directional solidification in refined Al-based alloys. *Journal of Alloys and Compounds*. 2009; 484:739-746. http://dx.doi.org/10.1016/j.jallcom.2009.05.029
23. Wu M, Fjeld A and Ludwig A. Modelling mixed columnar-equiaxed solidification with melt convection and grain sedimentation-Part I: Model description. *Computational Materials Science*. 2010; 50:32-42. http://dx.doi.org/10.1016/j.commatsci.2010.07.005
24. Wu M, Ludwig A and Fjeld A. Modelling mixed columnar-equiaxed solidification with melt convection and grain sedimentation-Part II: Illustrative modelling results and parameter studies. *Computational Materials Science*. 2010; 50:43-58. http://dx.doi.org/10.1016/j.commatsci.2010.07.006
25. Ares AE, Gueijman SF and Schvezov CE. An experimental investigation of the columnar-to-equiaxed grain transition in aluminum-copper hypoeutectic and eutectic alloys. *Journal of Crystal Growth*. 2010; 312:2154-2170. http://dx.doi.org/10.1016/j.jcrysgro.2010.04.040
26. Gueijman SF, Schvezov CE and Ares AE. Vertical and horizontal directional solidification of Zn-Al and Zn-Ag diluted alloys. *Materials Transactions*. 2010; 51:1861-1870. http://dx.doi.org/10.2320/matertrans.M2010036
27. Martorano MA, Beckermann C and Gandin CA. A solutal interaction mechanism for the columnar-to-equiaxed transition in alloy solidification. *Metallurgical and Materials Transactions A*. 2003; 34A:1657-1674.
28. Spittle JA. Columnar to equiaxed grain transition in as solidified alloys. *International Materials Reviews*. 2006; 51:247-269. http://dx.doi.org/10.1179/174328006X102493
29. Kaya H, Çadirli E, Gündüz M and Ülgen A. Effect of the temperature gradient, growth rate, and the interflake spacing on the microhardness in the directionally solidified Al-Si eutectic alloy. *Journal of Materials Engineering and Performance*. 2003; 12(5):544-551. http://dx.doi.org/10.1361/105994903100277201

30. Gündüz M, Kaya H, Çadirli E and Özmen A. Interflake spacings and undercoolings in Al–Si irregular eutectic alloy. *Materials Science and Engineering A* 2004; 369:215-229. http://dx.doi.org/10.1016/j.msea.2003.11.020

31. Peres MD, Siqueira CA and Garcia A. Macrostructural and microstructural development in Al-Si alloys directionally solidified under unsteady-state conditions. *Journal of Alloys and Compounds*. 2004; 381:168-181. http://dx.doi.org/10.1016/j.jallcom.2004.03.107

32. Santos CA, Quaresma JMV and Garcia A. Determination of transient interfacial heat transfer coefficients in chill mold castings. *Journal of Alloys and Compounds*. 2001; 319:174-186. http://dx.doi.org/10.1016/S0925-8388(01)00904-5

33. Spinelli JE, Ferreira IL and Garcia A. Evaluation of heat transfer coefficients during upward and downward transient directional solidification of Al-Si alloys. *Structural and Multidisciplinary Optimization*. 2006; 31:241-248. http://dx.doi.org/10.1007/s00158-005-0562-9

34. Ferreira IL, Spinelli JE, Nestler B and Garcia A. Influences of solute content, melt superheat and growth direction on the transient metal/mold interfacial heat transfer coefficient during solidification of Sn-Pb alloys. *Materials Chemistry and Physics*. 2008; 111:444-454. http://dx.doi.org/10.1016/j.matchemphys.2008.04.044

35. Cheung N, Ferreira IL, Pariona MM, Quaresma JMV and Garcia A. Melt characteristics and solidification growth direction with respect to gravity affecting the interfacial heat transfer coefficient of chill castings. *Materials and Design*. 2009; 30:3592-3601. http://dx.doi.org/10.1016/j.matdes.2009.02.025

36. Silva JN, Moutinho DJ, Moreira AL, Ferreira IL and Rocha OL. Determination of heat transfer coefficients at metal-mold interface during horizontal unsteady-state directional solidification of Sn-Pb alloys. *Materials Chemistry and Physics*. 2011; 130:179-185. http://dx.doi.org/10.1016/j.matchemphys.2011.06.032

37. Cheung N, Santos NS, Quaresma JMV, Dulikravich GS and Garcia A. Interfacial heat transfer coefficients and solidification of an aluminum alloy in a rotary continuous caster. *International Journal of Heat and Mass Transfer*. 2009; 52:451-459. http://dx.doi.org/10.1016/j.ijheatmasstransfer.2008.07.003

38. Gandin CA. Experimental study of the transition from constrained to unconstrained growth during directional solidification. *ISIJ International*. 2000; 40:971-979. http://dx.doi.org/10.2355/isijinternational.40.971

39. Magnusson T and Arnberg L. Density and solidification shrinkage of hypoeutectic aluminum-silicon alloys. *Metallurgical and Materials Transactions A*. 2001; 32A:2605-2613.

40. Bogno A, Nguyen-Thi H, Buffet A, Reinhart G, Billia B, Mangelinck-Noël N et al. Analysis by synchrotron x-ray radiography of convection effects on the dynamic evolution of the solid-liquid interface and on solute distribution during the initial transient of solidification. *Acta Materialia*. 2011; 59:4356-4365. http://dx.doi.org/10.1016/j.actamat.2011.03.059

41. Hellawell A, Liu S and Lu SZ. Dendrite fragmentation and the effects of fluid flow in castings. *Journal of the Minerals, Metals and Materials Society*. 1997; 49:18-20. http://dx.doi.org/10.1007/BF02914650